IEEE *Access*

Proactive Unmanned Aerial Vehicle Surveilling via Jamming in Decode-and-Forward Relay Networks

DINGKUN HU[1]**, QI ZHANG**[1]**, (Member, IEEE), QUANZHONG LI**[2]**, AND JIAYIN QIN**[1,3]

[1]School of Electronics and Information Technology, Sun Yat-sen University, Guangzhou 510006, China
[2]School of Data and Computer Science, Sun Yat-sen University, Guangzhou 510006, China
[3]Xinhua College, Sun Yat-sen University, Guangzhou 510520, China

Corresponding author: Qi Zhang (zhqi26@mail.sysu.edu.cn)

ABSTRACT Legitimately surveilling suspicious wireless communications is important for public security. In this paper, we propose a proactive legitimate unmanned aerial vehicle (UAV) monitor surveilling via a jamming scheme in suspicious decode-and-forward relay networks. To maximize average surveilling rate, we derive a closed-form optimal solution of jamming power given the position of the legitimate UAV monitor. With the derived optimal jamming power, we show that optimal position and jamming power are related to the height of the UAV monitor. Given the height of the UAV monitor, we theoretically prove that the optimal position of the monitor can be found by bisection search. From the numerical results, we show that the optimal position of the monitor found by bisection search achieves exactly the same average surveilling rate as that found by the 1-D search. It is also found that our proposed surveilling scheme with optimal position and jamming is superior to the surveilling scheme with a fixed position and the passive surveilling scheme.

INDEX TERMS Decode-and-forward (DF), proactive surveilling, relay networks, unmanned aerial vehicle (UAV).

I. INTRODUCTION

Infrastructure-free wireless communications, which may be misused by criminals or terrorists to commit crimes or launch terror attacks, brings new threats to public security [1]. To detect and stop such misuse, Xu *et al.* proposed proactive surveilling via jamming in [2], where how a legitimate monitor efficiently surveils a suspicious wireless communication link was investigated. In [3], that a legitimate monitor operates with simultaneous surveilling and spoofing relaying was studied. In [4], the surveilling non-outage probability was maximized for delay-sensitive suspicious wireless communication applications and the relative surveilling rate was maximized for delay-tolerant applications. In [5]–[8], proactive surveilling via jamming schemes for dual-hop amplify-and-forward (AF) and decode-and-forward (DF) relay networks were derived. In [9], the optimal transmit/receive beamforming vectors were obtained

considering four different scenarios, i.e., the legitimate monitor is equipped with single or multiple transmit antennas and single or multiple receive antennas. In [10], proactive surveilling via jamming over multiple-input-multiple-output (MIMO) Rayleigh fading channels was considered, where the suspicious source, the suspicious destination, and the legitimate monitor are equipped with multiple antennas. In [11], proactive surveilling model with multiple source-destination pairs was investigated. In [12]–[14], beamforming design problems for multi-antenna proactive surveilling were studied.

In [1]–[13], a legitimate monitor with fixed position was considered. A legitimate monitor mounted on an unmanned aerial vehicle (UAV) may achieve higher average surveilling rate [15], [16]. In the literature, UAV-based base station was proposed to improve wireless coverage in [17]. In [18], Zeng *et al.* proposed to use UAV in wireless relay networks. In [19], reinforcement learning was applied for an anti-jamming UAV relay network. In [20], UAVs were employed for mobile data collection. In [21] and [22], physical-layer

---

The associate editor coordinating the review of this manuscript and approving it for publication was Mehmet Alper Uslu.

security for UAV-based wireless communications were investigated. UAV-enabled mobile relays and cooperative jamming were considered to improve physical layer security in [23] and [24], respectively.

In [25], Lu *et al.* considered that a legitimate monitor tries to surveil on the suspicious messages sent by a UAV-aided suspicious transmitter. For proactive UAV surveilling, Li *et al.* proposed a wireless surveillance network in [26] which contains a legitimate UAV monitor and two suspicious UAVs. Furthermore, an energy-efficient jamming strategy was derived in [26].

Considering suspicious DF relay networks, we propose a proactive legitimate UAV monitor surveilling via jamming scheme in this paper. The scenario is typical for surveilling of suspicious device-to-device (D2D) wireless communications where two mobile devices communicate with the help of another mobile device [4], such as a fake base station. These infrastructure-free D2D communications are difficult to surveil utilizing conventional methods [4]. Thus, proactive legitimate surveilling by a UAV monitor may be suitable.

We consider that the legitimate UAV monitor accesses the DF relay network by pretending to be another relay node [6], [27]–[29]. Practically, this is implemented by the legitimate UAV monitor first eavesdropping the suspicious communications to acquire the key used for authentication and then joining the DF relay network as a fake relay node [27], [28]. Thus, the legitimate UAV monitor might be able to target the suspicious signals and acquire the locations of suspicious wireless nodes. The legitimate UAV monitor aims at continuously overhearing as much as possible suspicious signals by pretending to be a relay [1]–[10]. This is ensured by two facts. The former is suspicious signals can be continuously received by the suspicious destination under certain quality of service (QoS) constraint. Otherwise, either suspicious source always initiates retransmission or the legitimate surveillance is detected as well as suspicious transmission aborts. The latter is suspicious signals can be successfully decoded at the UAV monitor [1]–[10]. Thus, the UAV position over the suspicious source or suspicious relay does not always guarantee to be optimal.

In this paper, our goal is to maximize average surveilling rate by optimizing the position and jamming power of legitimate UAV monitor. To solve the problem, we derive the closed-form optimal solution of jamming power given the position of UAV monitor. Note that the jamming power optimization for proactive surveilling via jamming in decode-and-forward relay networks was also considered in [29], where all the channels are assumed to be known. However, in practice, the monitor is difficult to know the channels of suspicious links. In this paper, we only assume the channel from the monitor to the suspicious destination is known and derive the optimal jamming power. With the derived optimal jamming power, we will show that optimal position and jamming power are related with the height of UAV monitor. Given the height of UAV monitor, we theoretically prove that

the optimal position of monitor can be found by bisection search.

It is noted that the relay position optimization problem in conventional relay networks were extensively studied in the literature [30]–[39]. Unlike the relay position optimization problem, in the investigated problem here, the height of UAV monitor should be considered. For different heights of UAV monitor, the optimal positions of UAV monitor are different. Furthermore, in the investigated problem here, the proactive surveilling system is considered instead of conventional relay networks.

Our main contributions are listed as follows:
- Given the position of UAV monitor, we derive the closed-form optimal solution of jamming power;
- When the height of UAV monitor is lower than a specific value, we find that the optimal position of legitimate UAV monitor is over the suspicious source;
- When the height of UAV monitor is higher than a specific value, we theoretically prove that the one-dimensional search of the optimal position of legitimate UAV monitor can be replaced by the bisection search.

The rest of this paper is organized as follows. Section II describes the system model of proactive UAV surveilling via jamming in a DF relay network. In Section III, we propose joint position and jamming power optimization for proactive UAV surveilling where the optimal position of monitor is found by one-dimensional (1-D) search. In Section IV, we theoretically prove that the optimal position of monitor can be found by bisection search. We conclude the paper in Section V with a summary of our findings.

II. SYSTEM MODEL AND PROBLEM FORMULATION

As shown in Fig. 1, we investigate a proactive legitimate UAV monitor which surveils a suspicious DF relay network via jamming. The suspicious DF relay network is composed of a suspicious source (SS), a suspicious relay (SR), and a suspicious destination (SD). All the nodes have a single antenna. The direct link from SS to SD, assumed to be sufficiently weak, is neglected in this paper.
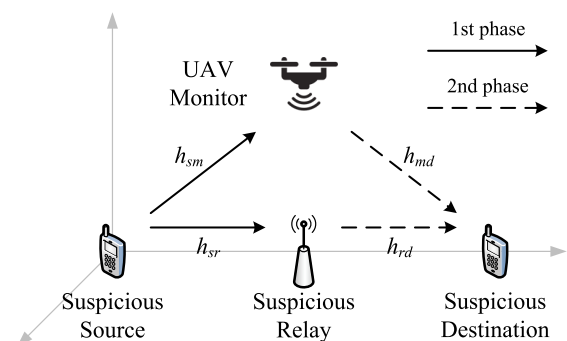

FIGURE 1. System model of proactive UAV surveilling via jamming in a DF relay network.

The suspicious DF relay network operates in a half-duplex mode. During the first phase, information signals, which are

transmitted from SS to SR, are also surveiled by the UAV monitor. During the second phase, the decoded signals at SR are forwarded to SD while jamming interferences are sent from UAV monitor to SD. If other legitimate destinations nearby operate at the same frequency, they will suffer co-channel interference temporarily.

We assume that the positions of SS, SR, and SD are fixed. The legitimate UAV monitor is assumed to fly at a fixed height H. Furthermore, the heights of SS, SR, and SD are negligible compared with that of the UAV monitor. Without loss of generality, the three-dimensional (3-D) coordinates of SS, SR, and SD are denoted as $\mathbf{w}_s = (0, 0, 0)^T$, $\mathbf{w}_r = (x_r, y_r, 0)^T$, and $\mathbf{w}_d = (x_d, 0, 0)^T$, respectively. The 3D coordinate of the UAV monitor is $\mathbf{w}_m = (x_m, y_m, H)^T$. The channel coefficients from SS to SR and UAV monitor are referred to as h_{sr} and h_{sm}, respectively. The channel coefficients from SR and UAV monitor to SD are referred to as h_{rd} and h_{md}, respectively. Here, flat block-fading Rayleigh fading wireless channels are considered. Therefore, $|h_{sr}|^2$, $|h_{sm}|^2$, $|h_{rd}|^2$, and $|h_{md}|^2$, are assumed to be independent exponential distributed random variables with parameters λ_{sr}, λ_{sm}, λ_{rd}, and λ_{md}, respectively. The parameters λ_{sr}, λ_{sm}, λ_{rd}, and λ_{md} are modeled by [37]–[40]

$$\lambda_{ij} = \|\mathbf{w}_i - \mathbf{w}_j\|^\nu \tag{1}$$

for $i \in \{s, r, m\}$ and $j \in \{r, m, d\}$, where $\nu \geq 2$ denotes the path loss factor. Thus, the channel gain $g_{ij} = |h_{ij}|^2$, $i \in \{s, r, m\}$, $j \in \{r, m, d\}$, has the probability density function (PDF)

$$f_{g_{ij}}(x) = \begin{cases} \lambda_{ij} \exp(-\lambda_{ij}x); & x \geq 0, \\ 0; & x < 0. \end{cases} \tag{2}$$

Since the SS, SR, and SD are assumed to be fixed, λ_{sr} and λ_{rd} are constant whereas λ_{sm} and λ_{md} are variables.

In the first phase, when the information signal s was transmitted from SS where $\mathbb{E}[|s|^2] = 1$, we have the received signals at SR and UAV monitor as follows

$$y_r = \sqrt{P_s} h_{sr} s + n_r, \tag{3}$$
$$y_m = \sqrt{P_s} h_{sm} s + n_m, \tag{4}$$

respectively, where $n_r \sim \mathcal{CN}(0, \sigma_r^2)$ and $n_m \sim \mathcal{CN}(0, \sigma_m^2)$ refer to the additive Gaussian noises at SR and UAV monitor, respectively, and P_s refers to transmitting power at SS.

In the second phase, the decoded signals at SR are forwarded to SD. We have the received signals at SD as follows

$$y_d = \sqrt{P_r} h_{rd} s + \sqrt{P_m} h_{md} z + n_d \tag{5}$$

where P_r refers to transmitting power at SR, $z \sim \mathcal{CN}(0, 1)$ refers to the jamming interference broadcasted by UAV monitor, P_m refers to transmitting power at UAV monitor, and $n_d \sim \mathcal{CN}(0, \sigma_d^2)$ refers to the additive Gaussian noise at SD.

Thus, the achievable rates of suspicious link from SS to SD and surveilling link from SS to UAV monitor are

$$r_s = \frac{1}{2} \log_2(1 + \varphi_s), \tag{6}$$
$$r_m = \frac{1}{2} \log_2(1 + \varphi_m), \tag{7}$$

respectively, where

$$\varphi_s = \min\left(\frac{P_s g_{sr}}{\sigma_r^2}, \frac{P_r g_{rd}}{P_m g_{md} + \sigma_d^2} \right), \tag{8}$$
$$\varphi_m = \frac{P_s g_{sm}}{\sigma_m^2}. \tag{9}$$

Here, that UAV monitor knows g_{md} is assumed. The assumption is suitable because g_{md} may be evaluated by the UAV monitor from two-way information exchanges between SS and SD employing property of channel reciprocal if time-division duplex (TDD) is employed [41]–[43]. After some mathematical manipulations, we have

$$\varphi_s = \min\left(\gamma_{sr}, \frac{\gamma_{rd}}{\gamma_{md} + 1} \right) \tag{10}$$

where

$$\gamma_{sr} = \frac{P_s g_{sr}}{\sigma_r^2}, \ \gamma_{rd} = \frac{P_r g_{rd}}{\sigma_d^2}, \text{ and } \gamma_{md} = \frac{P_m g_{md}}{\sigma_d^2}. \tag{11}$$

We assume that the existence of UAV monitor is not known at SS. The SS employs a fixed transmission rate, denoted as τ, for signal transmission [2]. During the transmission, if τ is less than or equal to the achievable rate r_s (r_m), the SD (the UAV monitor) can decode the signals sent from the SS correctly. Otherwise, the SD (the UAV monitor) cannot decode the signals correctly, i.e., a suspicious decoding (legitimate surveilling) outage happens. Thus, the suspicious decoding and legitimate surveilling outage probabilities at SD and the UAV monitor are

$$\zeta_s = \Pr(r_s < \tau), \tag{12}$$
$$\zeta_m = \Pr(r_m < \tau), \tag{13}$$

respectively.

In this paper, the average surveilling rate at the UAV monitor for a long period is defined as [2]

$$R_m \triangleq \tau(1 - \zeta_m). \tag{14}$$

The value of R_m provides us the amount of information bits/Hz per second be surveiled without decoding errors. Practically, the transmission rate τ of SS is controlled such that the suspicious decoding outage probability ζ_s is stabilized at a predefined threshold, i.e., $\zeta_s = \delta$, where $\delta > 0$ refers to the suspicious decoding outage probability threshold. If $\zeta_s < \delta$, SS will increase the transmission rate τ since SS is required to transmit information signals at its maximum allowable transmission rate under the quality of service (QoS) constraint. If $\zeta_s > \delta$, SS will decrease the transmission rate τ since SS should satisfy the QoS constraint. On the other hand, the UAV monitor may evaluate the value of δ from the

retransmission rate of SS for a long period. Thus, the UAV monitor can optimize its position and control P_m to reduce the achievable rate of suspicious link from SS to SD, r_s, thus reducing the suspicious transmission rate τ to keep $\zeta_s = \delta$ [2]. In this paper, our goal is to design the position of UAV monitor and control P_m to optimize the average surveilling rate at UAV monitor, R_m. Thus, we express the optimization problem as follows

$$\max_{\mathbf{w}_m, P_m} R_m$$
$$\text{s.t.} \quad \zeta_s = \delta, \ 0 \leq P_m \leq P_m^{\max} \quad (15)$$

where $P_m^{\max}$ refers to maximum allowable transmitting power at the UAV monitor.

Remark 1: In this paper, we assume that the UAV flies at a fixed height H above the ground. This is due to the minimum altitude required for safety. If H is also an optimization variable, the optimal value is $H = 0$.

Remark 2: From (14), the average surveilling rate R_m is related with τ and $(1 - \zeta_m)$. In Section III, we illustrate that τ is a monotonically decreasing function of P_m. From (14), $(1 - \zeta_m)$ is a monotonically increasing function of P_m. Therefore, there may exist an optimal P_m which maximizes R_m.

Remark 3: In this paper, the non-line-of-sight (NLoS) links and flat block-fading Rayleigh fading wireless channels are considered. This is because the suspicious transmission may happen in the day or night. If it happens in the day, the UAV monitor should be kept undiscovered, i.e., without the line-of-sight (LoS) to the SS, the SR, and the SD. Thus, the assumption of Rayleigh fading channels between the UAV monitor to the SS, the SR, and the SD is proper. If the suspicious transmission happens in the night, the channels between the UAV monitor to the SS, the SR, and the SD may be modeled as Rician fading channels. With the Rician fading assumption, the investigation of proactive UAV surveilling via jamming is an interesting future work.

Remark 4: In this paper, only the position of UAV monitor is optimized whereas the movement of UAV monitor during its surveillance is not considered. Intuitively, the UAV monitor may move towards the SS for better surveillance, and move towards the SD for better jamming. However, the time duration required for the change of UAV flying direction is generally much larger than the shifting of the first and second transmission phases in wireless relay networks. Whether both the position and the movement of UAV should be jointly optimized is an interesting future work.

Remark 5: In [11], proactive surveilling model with multiple source-destination pairs was investigated. The investigation on proactive UAV surveilling via jamming with multiple source-destination pairs is an interesting future work. In [12]–[14], the monitor equipped with multiple antennas was considered and beamforming design problems were solved. The study on proactive UAV surveilling via jamming where the monitor equipped with multiple antennas is also an interesting future work.

III. POSITION AND JAMMING POWER OPTIMIZATION FOR PROACTIVE UAV SURVEILLING
A. JAMMING POWER OPTIMIZATION
In this subsection, under the condition that $\mathbf{w}_m$ is given, we optimize P_m. In problem (15), the constraint $\zeta_s = \delta$ is equivalent to

$$F_{\varphi_s}(2^{2\tau} - 1) - \delta = 0 \quad (16)$$

where $F_X(x)$ refers to the cumulative distribution function (CDF) of random variable X. From (8), we obtain

$$F_{\varphi_s}(2^{2\tau} - 1) = 1 - \exp\left(-\xi\left(2^{2\tau} - 1\right)\right) \quad (17)$$

where

$$\xi = \sigma_r^2 \lambda_{sr}/P_s + \lambda_{rd}(P_m g_{md} + \sigma_d^2)/P_r. \quad (18)$$

Substituting (17) into (16), we have

$$\tau = \frac{1}{2}\log_2\left(1 + \frac{c}{\xi}\right) \quad (19)$$

where $c = -\ln(1 - \delta)$. From (19), τ is a monotonically decreasing function of P_m. From the constraint $0 \leq P_m \leq P_m^{\max}$, we obtain

$$\tau(P_m^{\max}) \leq \tau \leq \tau(0). \quad (20)$$

Substituting (7) into (13), we have

$$\zeta_m = \mathbb{P}\left(g_{sm} < \left(2^{2\tau} - 1\right)\sigma_m^2/P_s\right). \quad (21)$$

Given $\mathbf{w}_m = (x_m, y_m, H)^T$, substituting (1) and (2) into (21), we obtain

$$\zeta_m = 1 - \exp\left(-\left(x_m^2 + y_m^2 + H^2\right)^{\nu/2} \cdot \left(2^{2\tau} - 1\right)\sigma_m^2/P_s\right). \quad (22)$$

Thus, problem (15) can be transformed into

$$\max_{\tau} \ \tau \exp\left(-\left(x_m^2 + y_m^2 + H^2\right)^{\nu/2} \cdot \left(2^{2\tau} - 1\right)\sigma_m^2/P_s\right)$$
$$\text{s.t.} \ \tau(P_m^{\max}) \leq \tau \leq \tau(0). \quad (23)$$

From [2], problem (23) has the optimal solution as follows

$$\tau^* = \max\left(\min\left(\tau(0), \hat{\tau}\right), \tau(P_m^{\max})\right) \quad (24)$$

where $\hat{\tau}$ denotes the optimal solution to following problem $\max_{\tau} \tau \exp\left(-(x_m^2 + y_m^2 + H^2)^{\nu/2} \cdot (2^{2\tau} - 1)\sigma_m^2/P_s\right)$, i.e.,

$$\hat{\tau} = \frac{1}{2\ln 2}\mathcal{W}\left(\frac{P_s}{\sigma_m^2(x_m^2 + y_m^2 + H^2)^{\nu/2}}\right) \quad (25)$$

in which $\mathcal{W}(x)$ refers to the Lambert $\mathcal{W}$ function of x.

If the obtained τ^* is substituted into (19), the optimal jamming power is

$$P_m^* = \max\left(0, \min\left(\hat{P}_m, P_m^{\max}\right)\right) \quad (26)$$

where

$$\hat{P}_m = \frac{1}{g_{md}}\left(\frac{P_r}{\lambda_{rd}}\left(\frac{c}{2^{2\tau^*} - 1} - \frac{\sigma_r^2 \lambda_{sr}}{P_s}\right) - \sigma_d^2\right). \quad (27)$$

B. POSITION OPTIMIZATION

In the previous subsection, we obtain the closed-form expression of the optimal jamming power P_m^* which is a function of $\mathbf{w}_m$. In this subsection, we optimize the position of legitimate UAV monitor.

In (26), P_m^* is obtained under the assumption that g_{md} is known. From (1), the PDF of g_{md} is also a function of $\mathbf{w}_m$. Thus, we rewrite g_{md} as

$$g_{md} = \frac{\psi}{\|\mathbf{w}_m - \mathbf{w}_d\|^\nu} \qquad (28)$$

where ψ is a random variable whose PDF is

$$f_\psi(x) = \exp(-x)u(x). \qquad (29)$$

From (29), the PDF of ψ is not a function of $\mathbf{w}_m$. Substituting (28) into (27), we obtain

$$\hat{P}_m = \frac{1}{\psi} \left((x_m - x_d)^2 + y_m^2 + H^2 \right)^{\nu/2}$$

$$\cdot \left(\frac{P_r}{\lambda_{rd}} \left(\frac{c}{2^{2\tau^*} - 1} - \frac{\sigma_r^2 \lambda_{sr}}{P_s} \right) - \sigma_d^2 \right) \qquad (30)$$

where ψ is known to the UAV monitor.

To proceed, we need the following two lemmas.

Lemma 1: For the optimal position of legitimate UAV monitor, we have $y_m = 0$ and $0 \leq x_m \leq x_d$.

Proof: We prove Lemma 1 by contradiction. Suppose that the optimal position of UAV monitor is $(\tilde{x}_m, \tilde{y}_m, H)$, $\tilde{y}_m \neq 0$. The corresponding suspicious transmission rate and jamming power are denoted as $\tilde{\tau}_1$ and $\tilde{P}_1$. Consider another position of UAV monitor, $(\tilde{x}_m, 0, H)$. At this position, from (19), we can find a $\tilde{\tau}_2$ and a corresponding $\tilde{P}_2$ such that $\tilde{\tau}_2 = \tilde{\tau}_1$ and $\tilde{P}_2 \leq \tilde{P}_1$. From the objective function of problem (23), when $\tau = \tilde{\tau}_2 = \tilde{\tau}_1$ and $x_m = \tilde{x}_m$, the average surveilling rate is a monotonically decreasing function of $|y_m|$. Thus, the average surveilling rate at $(\tilde{x}_m, \tilde{y}_m, H)$ is less than that at $(\tilde{x}_m, 0, H)$. This contradicts with that the optimal position of UAV monitor is $(\tilde{x}_m, \tilde{y}_m, H)$. For $0 \leq x_m \leq x_d$, the proof is similar. ∎

From Lemma 1, for the optimal position of UAV monitor, only variable is x_m with the constraint $0 \leq x_m \leq x_d$.

Lemma 2: Denote $\tilde{R}_m(x_m)$ as the optimal objective value to the following problem

$$\max_{P_m \geq 0} R_m \text{ s.t. } \zeta_s = \delta \qquad (31)$$

given $\mathbf{w}_m = (x_m, 0, H)^T$. Denote $x_{m,1}$ and $x_{m,2}$ as two different values of x_m, with $x_{m,1} < x_{m,2}$. We have $\tilde{R}_m(x_{m,1}) > \tilde{R}_m(x_{m,2})$.

Proof: See Appendix A. ∎

From Lemma 2, if $\hat{\tau}$ in (25) satisfies $\tau(P_m^{\max}) \leq \hat{\tau} \leq \tau(0)$ for $0 \leq x_m \leq x_d$, the optimal position of UAV monitor is $x_m^* = 0$. Thus, we should discuss when the conditions $\tau(P_m^{\max}) \leq \hat{\tau} \leq \tau(0)$ are satisfied, especially for the special position $\mathbf{w}_m = (0, 0, H)^T$.

Denote $\hat{\tau}(x_m, H)$ as the obtained value of $\hat{\tau}$ by substituting $(x_m, y_m = 0, H)$ into (25). From (25), we know

$\hat{\tau}(0, 0) = +\infty$ and $\hat{\tau}(0, +\infty) = 0$. Substituting (28) and $y_m = 0$ into (19), we obtain

$$\tau(P_m, x_m, H) = \frac{1}{2} \log_2 \left(1 + \frac{c}{\kappa} \right) \qquad (32)$$

where

$$\kappa = \frac{\sigma_r^2 \lambda_{sr}}{P_s} + \frac{\lambda_{rd} \left(P_m \psi / \left((x_m - x_d)^2 + H^2 \right)^{\nu/2} + \sigma_d^2 \right)}{P_r}. \qquad (33)$$

From (32), we know $\tau(0, x_m, H) > 0$ is a constant for any x_m and H. Therefore, there exists a unique solution to $\tau(0, 0, H) = \hat{\tau}(0, H)$, which is denoted as H_1 since $\mathcal{W}(x)$ is monotonically increasing with respect to $x \geq 0$. The expression of H_1 is as follows

$$H_1 = \left(\frac{\sigma_m^2}{P_s} \left(1 + \frac{c}{\vartheta} \right) \ln \left(1 + \frac{c}{\vartheta} \right) \right)^{\frac{1}{\nu}}. \qquad (34)$$

where $\vartheta = \sigma_r^2 \lambda_{sr}/P_s + \lambda_{rd} \sigma_d^2 / P_r$.

Furthermore, $0 \leq \tau(P_m^{\max}, 0, 0) < \tau(P_m^{\max}, 0, +\infty)$. There also exists a unique solution to $\tau(P_m^{\max}, 0, H) = \hat{\tau}(0, H)$, which is denoted as H_2. Since $\tau(P_m, 0, H)$ is a monotonically decreasing function of P_m and $\hat{\tau}(0, H)$ is a monotonically decreasing function of H, we have $H_2 \geq H_1$. The value of H_2 can be obtained by the bisection search as we have proved. To continue, we need the following lemma.

Lemma 3: When $H > H_1$, the optimal jamming power P_m^* for any position $\mathbf{w}_m = (x_m, y_m, H)^T$ of legitimate UAV monitor is $P_m^* > 0$.

Proof: When $H > H_1$, $\hat{\tau}(0, H) < \tau(0, 0, H)$. Furthermore, since $\hat{\tau}(x_m, H)$ is a monotonically decreasing function of x_m given H, we have $\hat{\tau}(x_m, H) \leq \hat{\tau}(0, H)$ for $x_m > 0$. Thus, $\hat{\tau}(x_m, H) < \tau(0, 0, H) = \tau(0, x_m, H)$ because $\tau(0, x_m, H) > 0$ is a constant for any x_m and H. From (24), the optimal jamming power P_m^* for any position of UAV monitor is $P_m^* > 0$. ∎

Using Lemma 1, Lemma 2, and Lemma 3, we provide the optimal position of UAV monitor in following proposition.

Proposition 1: When $H \leq H_2$, the optimal position of legitimate UAV monitor is $\mathbf{w}_m^* = (0, 0, H)^T$. When $H > H_2$, the optimal position of legitimate UAV monitor is obtained by one-dimensional (1-D) search over $0 \leq x_m \leq x_d$ to find the maximum of

$$R_m(x_m, H) = \tau(P_m^{\max}, x_m, H)$$

$$\cdot \exp \left(- \left(x_m^2 + H^2 \right)^{\nu/2} \cdot \left(2^{2\tau(P_m^{\max}, x_m, H)} - 1 \right) \frac{\sigma_m^2}{P_s} \right). \qquad (35)$$

Proof: See Appendix B. ∎

IV. BISECTION SEARCH METHOD WHEN $H > H_2$

In the previous section, when $H > H_2$, the optimal position of legitimate UAV monitor is obtained by 1-D search over $0 \leq x_m \leq x_d$ to find the maximum of $R_m(x_m, H)$. Denote the first-order derivative of $R_m(x_m, H)$ with respect to x_m as $R_m'(x_m)$. If $R_m'(0) > 0$ and $R_m'(x_d) < 0$, there exists at least

a solution x_m to the equation $R'_m(x_m) = 0$. If the number of solutions to $R'_m(x_m) = 0$ is one, the only solution x_m achieves the maximum of $R_m(x_m, H)$. We can employ the bisection search method to find the solution x_m. The bisection search has lower computational complexity than the 1-D search.

To obtain the first-order derivative of $R_m(x_m, H)$, we find the first-order derivative of $\tau(P_m^{\max}, x_m, H)$ first. The first-order derivative of $\tau(P_m^{\max}, x_m, H)$ with respect to x_m, denoted as $\tau'(x_m)$, is

$$\tau'(x_m) = \frac{\lambda_{rd} P_m^{\max} \psi \nu}{P_r \cdot 2 \ln 2} \left(1 + \frac{c}{\kappa}\right)^{-1} \cdot \frac{c}{\kappa^2}$$
$$\cdot \left((x_m - x_d)^2 + H^2\right)^{\nu/2} \cdot (x_m - x_d). \quad (36)$$

It is noted that when $0 \le x_m < x_d$, $\tau'(x_m) < 0$ while when $x_m = x_d$, $\tau'(x_d) = 0$. Thus, the first-order derivative of $R_m(x_m, H)$ with respect to x_m, denoted as $R'_m(x_m)$, is

$$R'_m(x_m)$$
$$= \theta_{x_m} \tau'(x_m) - \frac{\theta_{x_m} \sigma_m^2 \ln \omega_{x_m}}{P_s \cdot 2 \ln 2} \left((x_m^2 + H^2)^{\nu/2 - 1}\right.$$
$$\left. \cdot \nu x_m (\omega_{x_m} - 1) + (x_m^2 + H^2)^{\nu/2} \omega_{x_m} \tau'(x_m) \cdot 2 \ln 2\right) \quad (37)$$

where

$$\theta_{x_m} = \exp\left(-\left(x_m^2 + H^2\right)^{\nu/2} \cdot \frac{\sigma_m^2 (\omega_{x_m} - 1)}{P_s}\right), \quad (38)$$

$$\omega_{x_m} = 2^{2\tau(P_m^{\max}, x_m, H)}. \quad (39)$$

When $x_m = 0$, we have

$$R'_m(0) = \theta_0 \tau'(0) \left(1 - \frac{\sigma_m^2 H^\nu \omega_0 \ln \omega_0}{P_s}\right). \quad (40)$$

Since $H > H_2$, we obtain

$$\tau(P_m^{\max}, 0, H) > \hat{\tau}(0, H) = \frac{1}{2 \ln 2} \mathcal{W}\left(\frac{P_s}{\sigma_m^2 H^\nu}\right). \quad (41)$$

Thus,

$$\omega_0 \ln \omega_0 > \mathcal{W}\left(\frac{P_s}{\sigma_m^2 H^\nu}\right) \exp\left(\mathcal{W}\left(\frac{P_s}{\sigma_m^2 H^\nu}\right)\right) = \frac{P_s}{\sigma_m^2 H^\nu}. \quad (42)$$

Since $\theta_0 > 0$ and $\tau'(0) < 0$, we have $R'_m(0) > 0$.

When $x_m = x_d$, since $\tau'(x_d) = 0$, we have

$$R'_m(x_d) = -\frac{\theta_{x_d} \sigma_m^2 \ln \omega_{x_d}}{P_s \cdot 2 \ln 2} (x_d^2 + H^2)^{\nu/2 - 1} \nu x_d (\omega_{x_d} - 1). \quad (43)$$

Since $\theta_{x_d} > 0$ and $\omega_{x_d} > 1$, we have $R'_m(x_d) < 0$.

Till now, we have proved that there exists at least a solution x_m to the equation $R'_m(x_m) = 0$. The possible number of solutions to $R'_m(x_m) = 0$ is one, three, five, $\cdots$, because $R'_m(0) > 0$ and $R'_m(x_d) < 0$. The following proposition will prove that the number of solutions to $R'_m(x_m) = 0$ is one and thus the bisection search method can be employed to find the optimal position of legitimate UAV monitor.

Proposition 2: The number of solutions to $R'_m(x_m) = 0$ is one.

Proof: See Appendix C. ∎

Complexity Analysis: For the proposed method to solve problem (15), when $H \le H_2$, we have derived the closed-form solution whose computational complexity is negligible. When $H > H_2$, if the bisection search method is employed, the computational complexity is

$$\mathcal{O}\left(\log_2\left(\frac{x_d}{\epsilon}\right)\right) \quad (44)$$

where ϵ denotes the bisection search accuracy.

V. NUMERICAL RESULTS

In the suspicious relay network, we assume that the 3D coordinates of SS, SR, and SD are $\mathbf{w}_s = (0, 0, 0)^T$, $\mathbf{w}_r = (500, 0, 0)^T$ and $\mathbf{w}_d = (1000, 0, 0)^T$, respectively, where the unit is meter [18]. We also assume that $\sigma_r^2 = \sigma_d^2 = \sigma_m^2 = -90$ dBm. The suspicious decoding outage probability threshold is $\delta = 0.2$ [2]. If not specified, the transmitting powers at SS and SR are $P_s = P_r = 10$ dBm [18]. The maximum allowable transmitting power at the legitimate UAV monitor is $P_m^{\max} = 20$ dBm [18]. The path loss factor is $\nu = 3$ [37]–[39].
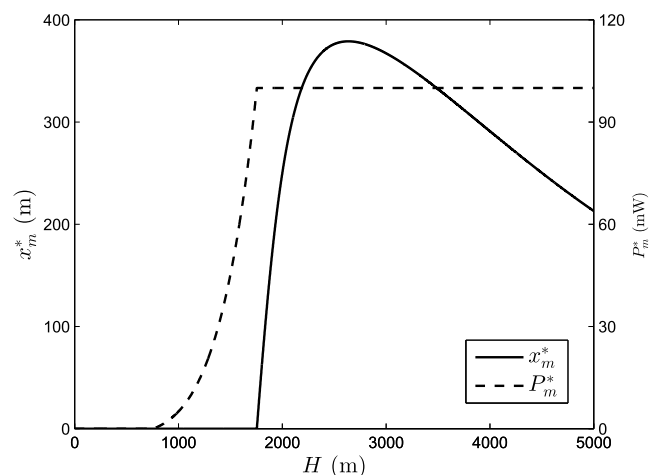
FIGURE 2. The optimal position of legitimate UAV monitor, x_m^*, and the optimal jamming power, P_m^*, with respect to the height of monitor, H.

In Fig. 2, we show the optimal position of UAV monitor, x_m^*, and the optimal jamming power, P_m^*, with respect to the height of monitor, H. We assume that $\psi = 1$. From Fig. 2, it is observed that H_1 is about 760 m and H_2 is about 1750 m. When $H \le H_1$, the optimal jamming power is $P_m^* = 0$ and the optimal position of UAV monitor is $x_m^* = 0$. When $H_1 < H \le H_2$, $0 < P_m^* \le 20$ dBm and $x_m^* = 0$. When $H > H_2$, $P_m^* = 20$ dBm and $x_m^* > 0$. When $H \to \infty$, the effect of jamming power on the suspicious DF relay network is negligible. Under this condition, from (32), $\tau(P_m, x_m, H)$ is a constant. Thus, from (35), the optimal position of UAV monitor, x_m^* converges to 0.

In Fig. 3, we present the average surveilling rate comparison of our proposed surveilling scheme with optimal
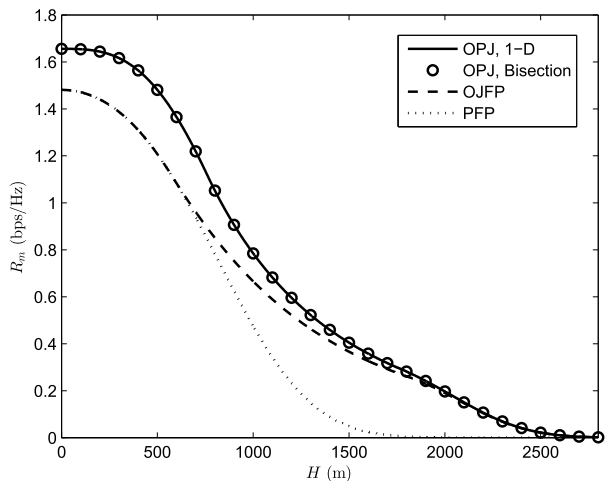
FIGURE 3. Average surveilling rate, R_m, versus H; performance comparison of the "OPJ, 1-D", "OPJ, Bisection", "OJFP", and "PFP" schemes.
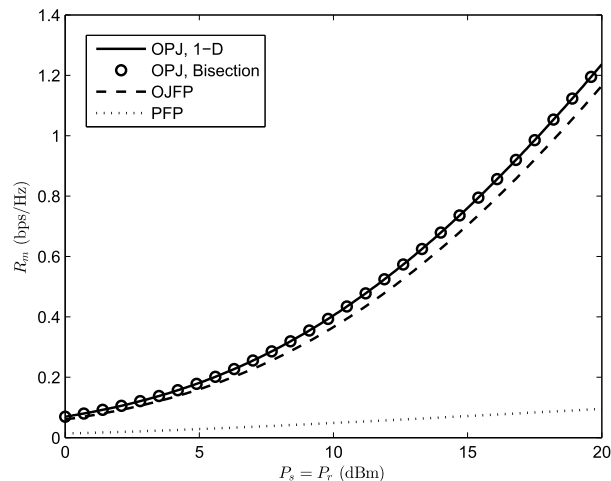

FIGURE 5. Average surveilling rate, R_m, versus $P_s = P_r$; performance comparison of the "OPJ, 1-D", "OPJ, Bisection", "OJFP", and "PFP" schemes where $H = 1500$ m and $P_m^{\max} = 20$ dBm.
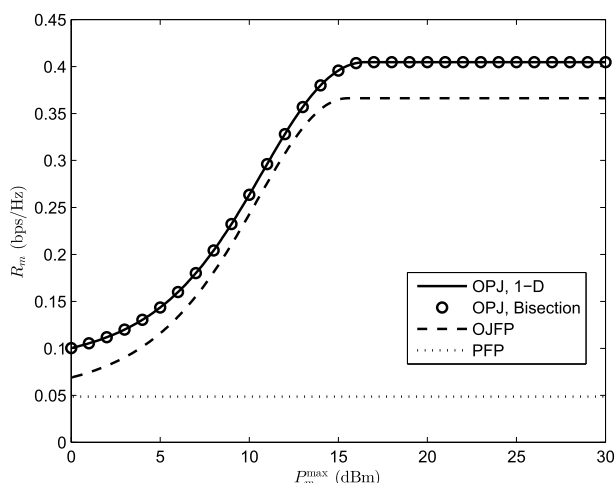

FIGURE 4. Average surveilling rate, R_m, versus $P_m^{\max}$; performance comparison of the "OPJ, 1-D", "OPJ, Bisection", "OJFP", and "PFP" schemes where $H = 1500$ m and $P_s = P_r = 10$ dBm.
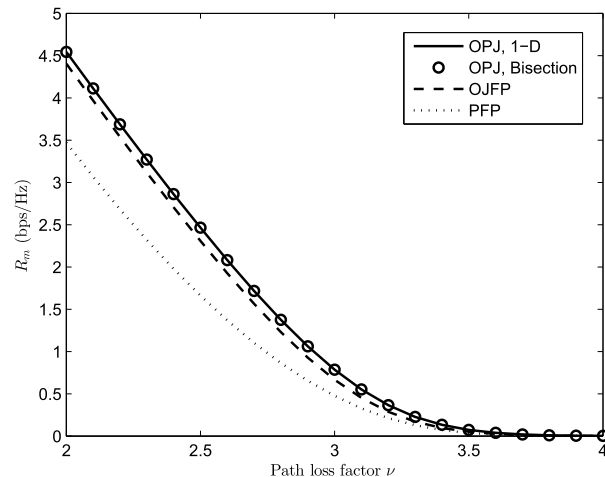

FIGURE 6. Average surveilling rate, R_m, versus the path loss factor v; performance comparison of the "OPJ, 1-D", "OPJ, Bisection", "OJFP", and "PFP" schemes where $H = 1000$ m, $P_s = P_r = 10$ dBm, and $P_m^{\max} = 20$ dBm.

position and jamming (denoted as "OPJ" in the legend) with other two schemes, i.e., surveilling with optimal jamming and fixed position, and passive surveilling with fixed position (denoted as "OJFP", and "PFP", respectively). For "OPJ" scheme, we present both results of 1-D search and bisection search (denoted as "1-D" and "Bisection", respectively). For both "OJFP" and "PFP" schemes, we assume that $\mathbf{w}_m = (500, 0, H)^T$. From Fig. 3, it is shown that the performance of our proposed "OPJ, Bisection" scheme is the same as that of "OPJ, 1-D" scheme and better than "OJFP" and "PFP" schemes. When $H = 500$ meter, our proposed schemes achieve the average surveilling rate of 1.48 bps/Hz whereas the "OJFP" scheme achieves 1.21 bps/Hz, which accounts for about 18.4% performance improvement. If the bandwidth is 100 MHz, the performance improvement is about 27 Mbps, which is not negligible.

In Fig. 4, we present the average surveilling rate comparison of the "OPJ, 1-D", "OPJ, Bisection", "OJFP", and

"PFP" schemes for different values of $P_m^{\max}$. Form Fig. 4, it is found that when $P_m^{\max}$ is higher than 17 dBm, the average surveilling rates of the "OPJ" and "OJFP" schemes remain the same. This is because $P_m^{\max}$ is higher than the optimal jamming powers. Form Fig. 4, it is also observed that the average surveilling rate of the "PFP" scheme remains a constant because passive surveilling scheme does not send jamming interference.

In Fig. 5, we present the average surveilling rate comparison of the "OPJ, 1-D", "OPJ, Bisection", "OJFP", and "PFP" schemes for different values of $P_s = P_r$ where $H = 1500$ m. Form Fig. 5, it is shown that with the increase of $P_s = P_r$, the average surveilling rates of the "OPJ", "OJFP", and "PFP" schemes increase. Furthermore, with the increase of $P_s = P_r$, the gap between the average surveilling rates of the "OPJ" and "OJFP" schemes also increases.

In Fig. 6, we present the average surveilling rate comparison of the "OPJ, 1-D", "OPJ, Bisection", "OJFP", and

"PFP" schemes for different values of path loss factor ν where $H = 1000$ m. Form Fig. 6, it is observed that with the increase of ν, the average surveilling rates of the "OPJ", "OJFP", and "PFP" schemes decrease.

VI. CONCLUSION

In this paper, we have proposed legitimate UAV surveilling scheme with optimal position and jamming where the optimal position of monitor is found by bisection search. It is shown through numerical results that the optimal position of monitor found by bisection search achieves exactly the same average surveilling rate as that found by 1-D search. It is also found that our proposed scheme performs better than the surveilling scheme with fixed position and the passive surveilling scheme.

APPENDIX A
PROOF OF LEMMA 2

Problem (31) can be equivalently rewritten as

$$\max_{\tau} \ \tau \exp\left(-\left(x_m^2 + H^2\right)^{\nu/2} \cdot \left(2^{2\tau} - 1\right)\frac{\sigma_m^2}{P_s}\right)$$
$$\text{s.t. } \tau \leq \tau(0). \tag{45}$$

The optimal solution to problem (45) is $\min\left(\tau(0), \hat{\tau}\right)$.

Substituting $x_{m,1}$ and $x_{m,2}$ into (45), if both optimal solutions to problem (45) are $\tau(0)$, we have

$$\tilde{R}_m(x_m) = \tau(0) \cdot \exp\left(-\left(x_m^2 + H^2\right)^{\nu/2} \cdot \left(2^{2\tau(0)} - 1\right)\frac{\sigma_m^2}{P_s}\right) \tag{46}$$

where

$$\tau(0) = \frac{1}{2}\log_2\left(1 + \frac{c}{\sigma_r^2\lambda_{sr}/P_s + \sigma_d^2\lambda_{rd}/P_r}\right). \tag{47}$$

From (46), $\tilde{R}_m(x_m)$ is a monotonically decreasing function of x_m. Thus, we obtain $\tilde{R}_m(x_{m,1}) > \tilde{R}_m(x_{m,2})$.

Substituting $x_{m,1}$ and $x_{m,2}$ into (45), if both optimal solutions to problem (45) are $\hat{\tau}$, we have

$$\tilde{R}_m(x_m) = \tilde{\tau}\exp\left(-\left(x_m^2 + H^2\right)^{\nu/2} \cdot \left(2^{2\tilde{\tau}} - 1\right)\frac{\sigma_m^2}{P_s}\right) \tag{48}$$

where

$$\tilde{\tau} = \frac{1}{2\ln 2}\mathcal{W}\left(\frac{P_s}{\sigma_m^2(x_m^2 + H^2)^{\nu/2}}\right). \tag{49}$$

Let

$$\mu = \frac{P_s}{\sigma_m^2(x_m^2 + H^2)^{\nu/2}}. \tag{50}$$

We have

$$\tilde{R}_m(x_m) = \frac{\mathcal{W}(\mu)}{2\ln 2}\exp\left(\frac{1 - \exp\left(\mathcal{W}(\mu)\right)}{\mu}\right). \tag{51}$$

Since $\mathcal{W}(\mu)\exp(\mathcal{W}(\mu)) = \mu$, we obtain

$$\tilde{R}_m(x_m) = \frac{\mathcal{W}(\mu)}{2\ln 2}\exp\left(\frac{1}{\mu} - \frac{1}{\mathcal{W}(\mu)}\right). \tag{52}$$

Using the property that $\frac{d}{d\mu}\mathcal{W}(\mu) = \frac{1}{1+\mathcal{W}(\mu)}$, we have

$$\frac{d}{d\mu}\tilde{R}_m(x_m) = \frac{1}{2\ln 2}\left(-\frac{\mathcal{W}(\mu)}{\mu^2} + \frac{1}{\mathcal{W}(\mu)}\right)$$
$$\cdot \exp\left(\frac{1}{\mu} - \frac{1}{\mathcal{W}(\mu)}\right). \tag{53}$$

When $\mu > 0$, $\mathcal{W}(\mu) > 0$ and $\exp(\mathcal{W}(\mu)) > 1$. Accordingly, $\mu/\mathcal{W}(\mu) > 1$ and $\mathcal{W}(\mu)/\mu^2 < 1/\mathcal{W}(\mu)$. Thus, $\tilde{R}_m(x_m)$ is a monotonically increasing function of μ. From (50), μ is a monotonically decreasing function of x_m because from Lemma 1, we have $0 \leq x_m \leq x_d$ for the optimal position of monitor. Therefore, $\tilde{R}_m(x_m)$ is a monotonically decreasing function of x_m. We obtain $\tilde{R}_m(x_{m,1}) > \tilde{R}_m(x_{m,2})$.

Substituting $x_{m,1}$ and $x_{m,2}$ into (45), suppose one optimal solution to problem (45) is $\tau(0)$ and the other is $\hat{\tau}$. Since $\hat{\tau}$ is a monotonically decreasing function of x_m and $x_{m,1} < x_{m,2}$, Thus, the optimal solution for $x_{m,1}$ to problem (45) is $\tau(0)$ and the optimal solution for $x_{m,2}$ is $\hat{\tau}$. Since the function $\hat{\tau}$ with respect to x_m is continuous, we have $x_{m,3}$ with $x_{m,1} \leq x_{m,3} \leq x_{m,2}$ which achieves the optimal solution that $\hat{\tau} = \tau(0)$ when substituted into (45). From (46), $\tilde{R}_m(x_{m,1}) > \tilde{R}_m(x_{m,3})$ and from (46), $\tilde{R}_m(x_{m,3}) > \tilde{R}_m(x_{m,2})$. Combing two inequality, we obtain $\tilde{R}_m(x_{m,1}) > \tilde{R}_m(x_{m,2})$.

APPENDIX B
PROOF OF PROPOSITION 1

It is noted that from Lemma 1, for the optimal position of UAV monitor, only variable is x_m with the constraint $0 \leq x_m \leq x_d$. We consider the following three cases.

Case I ($H \leq H_1$): In this case, all the positions of UAV monitor can be divided into two sets according to their optimal jamming power, P_m^*. Two sets are denoted as $\mathcal{M}_1$ and $\mathcal{M}_2$, whose optimal jamming power are $0 \leq P_m^* < P_m^{\max}$ and $P_m^* = P_m^{\max}$, respectively. Since $H \leq H_1$ and $\tau(0, 0, H) \leq \hat{\tau}(0, H)$, the optimal jamming power for $x_m = 0$ is $P_m^* = 0$. Thus, $x_m = 0 \in \mathcal{M}_1$.

For any position $x_m \in \mathcal{M}_2$, from (26), we have $\hat{P}_m \geq P_m^{\max}$. Define

$$\check{R}_m(x_m, P_m) = \max \ R_m \quad \text{s.t. } \zeta_s = \delta \tag{54}$$

given $\mathbf{w}_m = (x_m, 0, H)^T$ and P_m. We have $\check{R}_m(x_m, P_m^{\max}) < \check{R}_m(x_m, \hat{P}_m)$ because $\hat{P}_m$ is the solution to problem $\max_{P_m} \check{R}_m(x_m, P_m)$ and $P_m^{\max}$ is the solution to problem $\max_{P_m} \check{R}_m(x_m, P_m)$ s.t. $0 \leq P_m \leq P_m^{\max}$.

Define $\mathcal{M}_3 = \mathcal{M}_1 \cup \mathcal{M}_2$. From Lemma 2, $\tilde{R}_m(x_{m,1}) > \tilde{R}_m(x_{m,2})$ for $x_{m,1} < x_{m,2}$. Thus, the optimal x_m is the minimum in $\mathcal{M}_3$, i.e., $x_m^* = 0$.

Case II ($H_1 < H \leq H_2$): In this case, $x_m = 0 \in \mathcal{M}_1$. It is similar as Case I to prove that the optimal x_m is $x_m^* = 0$.

Case III ($H > H_2$): In this case, $\tau(P_m^{\max}, 0, H) > \hat{\tau}(0, H)$. Thus, $x_m = 0 \in \mathcal{M}_2$. Define $\mathcal{M}_4$ as a position set of UAV monitor whose optimal jamming power are $P_m^* = \hat{P}_m = P_m^{\max}$. It is noted that $\mathcal{M}_4 \in \mathcal{M}_2$. For $x_m \in \mathcal{M}_1 \cup \mathcal{M}_4$, from Lemma 2, the optimal x_m is the minimum in $\mathcal{M}_1 \cup \mathcal{M}_4$. Since $x_m = 0 \in \mathcal{M}_2$ and $\mathcal{M}_4$ constitutes the boundary of $\mathcal{M}_1$, the optimal x_m is the minimum in $\mathcal{M}_4$. Thus, for $0 \leq x_m \leq x_d$, the optimal x_m is in $\mathcal{M}_2$.

Substituting $P_m^{\max}$ into (19), we have

$$\tau(P_m^{\max}, x_m, H)$$
$$= \frac{1}{2\ln 2} \ln \left(1 + \frac{\alpha}{\beta + \left((x_m - x_d)^2 + H^2\right)^{-\nu/2}} \right) \quad (55)$$

where

$$\alpha = \frac{cP_r}{P_m^{\max} \psi \lambda_{rd}}, \quad (56)$$

$$\beta = \frac{P_r}{P_m^{\max} \psi \lambda_{rd}} \left(\frac{\sigma_r^2 \lambda_{sr}}{P_s} + \frac{\sigma_d^2 \lambda_{rd}}{P_r} \right). \quad (57)$$

Under this condition, the average surveilling rate given x_m and H is (35). Thus, the optimal position of UAV monitor is obtained by 1-D search over $0 \leq x_m \leq x_d$ to find the maximum of (35).

APPENDIX C
PROOF OF PROPOSITION 2

We rewrite the expression of $R_m'(x_m)$ as

$$R_m'(x_m) = \theta_{x_m} \Phi(x_m) \quad (58)$$

where

$$\Phi(x_m) = \tau'(x_m) \cdot \left(1 - \frac{\sigma_m^2 \ln \omega_{x_m}}{P_s}(x_m^2 + H^2)^{\nu/2} \omega_{x_m} \right)$$
$$- \frac{\sigma_m^2 \ln \omega_{x_m}}{P_s \cdot 2\ln 2}(x_m^2 + H^2)^{\nu/2-1} \nu x_m (\omega_{x_m} - 1). \quad (59)$$

Since $\theta_{x_m} > 0$, $R_m'(x_m) = 0$ means $\Phi(x_m) = 0$. To prove the number of solutions to $R_m'(x_m) = 0$ is one, i.e., the number of solutions to $R_m'(x_m) = 0$ is less than three, we compute the first-order derivative of $\Phi(x_m)$ with respect to x_m as follows

$$\Phi'(x_m) = \tau''(x_m) \cdot \Upsilon(x_m) - \Theta(x_m) \quad (60)$$

where

$$\tau''(x_m) = \frac{\lambda_{rd} P_m^{\max} \psi \nu}{P_r \cdot 2\ln 2} \left(1 + \frac{c}{\kappa} \right)^{-1} \cdot \frac{c}{\kappa^2}$$
$$\cdot \left((x_m - x_d)^2 + H^2\right)^{\nu/2}, \quad (61)$$

$$\Upsilon(x_m) = 1 - \frac{\sigma_m^2 \ln \omega_{x_m}}{P_s}(x_m^2 + H^2)^{\nu/2} \omega_{x_m}, \quad (62)$$

$$\Theta(x_m) = \frac{\sigma_m^2 \ln \omega_{x_m}}{P_s \cdot 2\ln 2}(x_m^2 + H^2)^{\nu/2-1} \nu(\omega_{x_m} - 1). \quad (63)$$

In the derivations, because when $H > H_2$, the variations of $(x_m^2 + H^2)^{\nu/2}$ and ω_{x_m}, κ, and $((x_m - x_d)^2 + H^2)^{\nu/2}$ are negligible compared with that of x_m, the derivatives of $(x_m^2 + H^2)^{\nu/2}$ and ω_{x_m}, κ, and $((x_m - x_d)^2 + H^2)^{\nu/2}$ with respect to x_m are omitted.

In (60), $\tau''(x_m) > 0$ and $\Theta(x_m) \geq 0$. Furthermore, the variations of $\tau''(x_m)$ and $\Theta(x_m)$ with respect to x_m are negligible. To find the property of $\Upsilon(x_m)$, we find the solution to the following equation

$$1 = \frac{\sigma_m^2 \ln \omega_{x_m}}{P_s}(x_m^2 + H^2)^{\nu/2} \omega_{x_m}. \quad (64)$$

The equation (64) is equivalent to

$$\omega_{x_m} \ln \omega_{x_m} = \frac{P_s}{\sigma_m^2 (x_m^2 + H^2)^{\nu/2}}. \quad (65)$$

From the property of Lambert $\mathcal{W}$ function, (65) is equivalent to $\rho(x_m) = 0$ where

$$\rho(x_m) = \tau(P_m^{\max}, x_m, H) - \frac{1}{2\ln 2}\mathcal{W}(\chi), \quad (66)$$

$$\chi = \frac{P_s}{\sigma_m^2 (x_m^2 + H^2)^{\nu/2}}. \quad (67)$$

Taking the first-order derivative of $\rho(x_m)$ with respect to x_m, we have

$$\rho'(x_m) = \tau'(x_m) + \frac{P_s \nu (x_m^2 + H^2)^{-\nu/2-1} x_m}{\sigma_m^2 (1 + \mathcal{W}(\chi)) 2\ln 2}. \quad (68)$$

In (68), when $H > H_2$, the variations of $\mathcal{W}(\chi)$ and $(x_m^2 + H^2)^{-\nu/2-1}$ are negligible compared with that of x_m. The second term in the right-hand side of (68) is a monotonically increasing function. $\tau'(x_m)$ is also a monotonically increasing function. Furthermore, $\rho'(0) < 0$ and $\rho'(x_d) > 0$. Thus, $\rho'(x_m) = 0$ has only one solution.

In (64), when $x_m = 0$, from (42),

$$\frac{\sigma_m^2}{P_s} H^\nu \omega_0 \ln \omega_0 > 1, \quad (69)$$

and thus $\Upsilon(x_m) < 0$. When x_m is close to zero, the variation of $(x_m^2 + H^2)^{\nu/2}$ is close to zero because

$$\frac{d(x_m^2 + H^2)^{\nu/2}}{dx_m} = \nu(x_m^2 + H^2)^{\nu/2-1} x_m. \quad (70)$$

Furthermore, $\omega_{x_m} \ln \omega_{x_m}$ is a monotonically decreasing function. Thus, when x_m is close to zero, $\Upsilon(x_m)$ decreases with the increase of x_m. Since $\rho'(x_m) = 0$ has only one solution, after an inflection point, $\Upsilon(x_m)$ will increase with the increase of x_m. This indicates that the number of solutions to $R_m'(x_m) = 0$ is one.

REFERENCES

[1] J. Xu, L. Duan, and R. Zhang, "Surveillance and intervention of infrastructure-free mobile communications: A new wireless security paradigm," *IEEE Wireless Commun.*, vol. 24, no. 4, pp. 152–159, Aug. 2017.

[2] J. Xu, L. Duan, and R. Zhang, "Proactive eavesdropping via jamming for rate maximization over Rayleigh fading channels," *IEEE Wireless Commun. Lett.*, vol. 5, no. 1, pp. 80–83, Feb. 2016.

[3] Y. Zeng and R. Zhang, "Wireless information surveillance via proactive eavesdropping with spoofing relay," *IEEE J. Sel. Topics Signal Process.*, vol. 10, no. 8, pp. 1449–1461, Dec. 2016.

[4] J. Xu, L. Duan, and R. Zhang, "Proactive eavesdropping via cognitive jamming in fading channels," *IEEE Trans. Wireless Commun.*, vol. 16, no. 5, pp. 2790–2806, May 2017.

[5] G. Ma, J. Xu, L. Duan, and R. Zhang, "Wireless surveillance of two-hop communications," Apr. 2017, *arXiv:1704.07629*. [Online]. Available: https://arxiv.org/abs/1704.07629

[6] J. Xu, L. Duan, and R. Zhang, "Transmit optimization for symbol-level spoofing," *IEEE Trans. Wireless Commun.*, vol. 17, no. 1, pp. 41–55, Jan. 2018.

[7] D. Hu, Q. Zhang, P. Yang, and J. Qin, "Proactive monitoring via jamming in amplify-and-forward relay networks," *IEEE Signal Process. Lett.*, vol. 24, no. 11, pp. 1714–1718, Nov. 2017.

[8] X. Jiang, H. Lin, C. Zhong, X. Chen, and Z. Zhang, "Proactive eavesdropping in relaying systems," *IEEE Signal Process. Lett.*, vol. 24, no. 6, pp. 917–921, Jun. 2017.

[9] C. Zhong, X. Jiang, F. Qu, and Z. Zhang, "Multi-antenna wireless legitimate surveillance systems: Design and performance analysis," *IEEE Trans. Wireless Commun.*, vol. 16, no. 7, pp. 4585–4599, Jul. 2017.

[10] H. Cai, Q. Zhang, Q. Li, and J. Qin, "Proactive monitoring via jamming for rate maximization over MIMO Rayleigh fading channels," *IEEE Commun. Lett.*, vol. 21, no. 9, pp. 2021–2024, Sep. 2017.

[11] B. Li, Y. Yao, H. Zhang, Y. Lv, and W. Zhao, "Energy efficiency of proactive eavesdropping for multiple links wireless system," *IEEE Access*, vol. 6, pp. 26081–26090, 2018.

[12] S. Huang, Q. Zhang, Q. Li, and J. Qin, "Robust proactive monitoring via jamming with deterministically bounded channel errors," *IEEE Signal Process. Lett.*, vol. 25, no. 5, pp. 690–694, May 2018.

[13] M. Zhu, J. Mo, N. Xiong, and J. Wang, "Legitimate monitoring via cooperative relay and proactive jamming," *IEEE Access*, vol. 7, pp. 40133–40143, 2019.

[14] Y. Cai, C. Zhao, Q. Shi, G. Y. Li, and B. Champagne, "Joint beamforming and jamming design for mmWave information surveillance systems," *IEEE J. Sel. Areas Commun.*, vol. 36, no. 7, pp. 1410–1425, Jul. 2018.

[15] M. Mozaffari, W. Saad, M. Bennis, and M. Debbah, "Unmanned aerial vehicle with underlaid device-to-device communications: Performance and tradeoffs," *IEEE Trans. Wireless Commun.*, vol. 15, no. 6, pp. 3949–3963, Jun. 2016.

[16] Y. Zeng, R. Zhang, and T. J. Lim, "Wireless communications with unmanned aerial vehicles: Opportunities and challenges," *IEEE Commun. Mag.*, vol. 54, no. 5, pp. 36–42, May 2016.

[17] J. Lyu, Y. Zeng, R. Zhang, and T. J. Lim, "Placement optimization of UAV-mounted mobile base stations," *IEEE Commun. Lett.*, vol. 21, no. 3, pp. 604–607, Mar. 2017.

[18] Y. Zeng, R. Zhang, and T. J. Lim, "Throughput maximization for UAV-enabled mobile relaying systems," *IEEE Trans. Commun.*, vol. 64, no. 12, pp. 4983–4996, Dec. 2016.

[19] L. Xiao, X. Lu, D. Xu, Y. Tang, L. Wang, and W. Zhuang, "UAV relay in VANETs against smart jamming with reinforcement learning," *IEEE Trans. Veh. Technol.*, vol. 67, no. 5, pp. 4087–4097, May 2018.

[20] J. Lyu, Y. Zeng, and R. Zhang, "Cyclical multiple access in UAV-aided communications: A throughput-delay tradeoff," *IEEE Wireless Commun. Lett.*, vol. 5, no. 6, pp. 600–603, Dec. 2016.

[21] M. Cui, G. Zhang, Q. Wu, and D. W. K. Ng, "Robust trajectory and transmit power design for secure UAV communications," *IEEE Trans. Veh. Technol.*, vol. 67, no. 9, pp. 9042–9046, Sep. 2018.

[22] G. Zhang, Q. Wu, M. Cui, and R. Zhang, "Securing UAV communications via joint trajectory and power control," *IEEE Trans. Wireless Commun.*, vol. 18, no. 2, pp. 1376–1389, Feb. 2019.

[23] Q. Wang, Z. Chen, W. Mei, and J. Fang, "Improving physical layer security using UAV-enabled mobile relaying," *IEEE Wireless Commun. Lett.*, vol. 6, no. 3, pp. 310–313, Jun. 2017.

[24] H. Lee, S. Eom, J. Park, and I. Lee, "UAV-aided secure communications with cooperative jamming," *IEEE Trans. Veh. Commun.*, vol. 67, no. 10, pp. 9385–9392, Oct. 2018.

[25] H. Lu, H. Zhang, H. Dai, W. Wu, and B. Wang, "Proactive eavesdropping in UAV-aided suspicious communication systems," *IEEE Trans. Veh. Technol.*, vol. 68, no. 2, pp. 1993–1997, Feb. 2019.

[26] K. Li, R. C. Voicu, S. S. Kanhere, W. Ni, and E. Tovar, "Energy efficient legitimate wireless surveillance of UAV communications," *IEEE Trans. Veh. Technol.*, vol. 68, no. 3, pp. 2283–2293, Mar. 2019.

[27] Y. Zou, J. Zhu, X. Wang, and L. Hanzo, "A survey on wireless security: Technical challenges, recent advances, and future trends," *Proc. IEEE*, vol. 104, no. 9, pp. 1727–1765, Sep. 2016.

[28] B. Kannhavong, H. Nakayama, Y. Nemoto, N. Kato, and A. Jamalipour, "A survey of routing attacks in mobile ad hoc networks," *IEEE Wireless Commun.*, vol. 14, no. 5, pp. 85–91, Oct. 2007.

[29] Y. Zhang, X. Jiang, C. Zhong, and Z. Zhang, "Performance of proactive eavesdropping in dual-hop relaying systems," in *Proc. IEEE Globecom Workshops*, Dec. 2017, pp. 1–6.

[30] W. Guo and T. O'Farrell, "Relay deployment in cellular networks: Planning and optimization," *IEEE J. Sel. Areas Commun.*, vol. 31, no. 8, pp. 1597–1606, Aug. 2013.

[31] M. Minelli, M. Ma, M. Coupechoux, J.-M. Kelif, M. Sigelle, and P. Godlewski, "Optimal relay placement in cellular networks," *IEEE Trans. Wireless Commun.*, vol. 13, no. 2, pp. 998–1009, Feb. 2014.

[32] M. Minelli, M. Ma, M. Coupechoux, J.-M. Kelif, M. Sigelle, and P. Godlewski, "Uplink energy-delay trade-off under optimized relay placement in cellular networks," *IEEE Trans. Mobile Comput.*, vol. 15, no. 9, pp. 2376–2387, Sep. 2016.

[33] F. Parzysz, M. Vu, and F. Gagnon, "Impact of propagation environment on energy-efficient relay placement: Model and performance analysis," *IEEE Trans. Wireless Commun.*, vol. 13, no. 4, pp. 2214–2228, Apr. 2014.

[34] F. Parzysz, M. Vu, and F. Gagnon, "Modeling and analysis of energy efficiency and interference for cellular relay deployment," *IEEE Trans. Wireless Commun.*, vol. 16, no. 2, pp. 982–997, Feb. 2017.

[35] M. Nikolov and Z. J. Haas, "Relay placement in wireless networks: Minimizing communication cost," *IEEE Trans. Wireless Commun.*, vol. 15, no. 5, pp. 3587–3602, May 2016.

[36] A. D. Mafuta, T. Walingo, and T. M. N. Ngatched, "Energy efficient coverage extension relay node placement in LTE-A networks," *IEEE Commun. Lett.*, vol. 21, no. 7, pp. 1617–1620, Jul. 2017.

[37] J. Mo, M. Tao, and Y. Liu, "Relay placement for physical layer security: A secure connection perspective," *IEEE Commun. Lett.*, vol. 16, no. 6, pp. 878–881, Jun. 2012.

[38] B. Yu, L. Yang, X. Cheng, and R. Cao, "Power and location optimization for full-duplex decode-and-forward relaying," *IEEE Trans. Commun.*, vol. 63, no. 12, pp. 4743–4753, Dec. 2015.

[39] S. Liu, S. Jin, H. Zhu, and K.-K. Wong, "On impact of relay placement for energy-efficient cooperative networks," *IET Commun.*, vol. 8, no. 1, pp. 140–151, Jan. 2014.

[40] A. A. Nasir, X. Zhou, S. Durrani, and R. A. Kennedy, "Relaying protocols for wireless energy harvesting and information processing," *IEEE Trans. Wireless Commun.*, vol. 12, no. 7, pp. 3622–3636, Jul. 2013.

[41] R. Wang and M. Tao, "Joint source and relay precoding designs for MIMO two-way relaying based on MSE criterion," *IEEE Trans. Signal Process.*, vol. 60, no. 3, pp. 1352–1365, Mar. 2012.

[42] F. Gao, T. Cui, and A. Nallanathan, "On channel estimation and optimal training design for amplify and forward relay networks," *IEEE Trans. Wireless Commun.*, vol. 7, no. 5, pp. 1907–1916, May 2008.

[43] F. Gao, R. Zhang, and Y.-C. Liang, "Optimal channel estimation and training design for two-way relay networks," *IEEE Trans. Commun.*, vol. 57, no. 10, pp. 3024–3033, Oct. 2009.
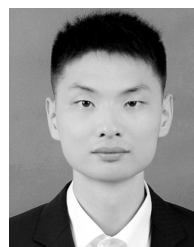
DINGKUN HU received the B.Eng. degree in communication engineering from the Wuhan University of Technology, Wuhan, China, in 2016. He is currently pursuing the M.S. degree with the School of Electronics and Information Technology, Sun Yat-sen University, Guangzhou, China. His research interests include UAV communications, non-orthogonal multiple access, and cooperative communications.
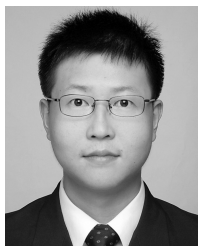
QI ZHANG (S'04–M'11) received the B.Eng. (Hons.) and M.S. degrees from the University of Electronic Science and Technology of China, Chengdu, China, in 1999 and 2002, respectively, and the Ph.D. degree in electrical and computer engineering from the National University of Singapore (NUS), Singapore, in 2007.

From 2007 to 2008, he was a Research Fellow with the Communications Laboratory, Department of Electrical and Computer Engineering, NUS. From 2008 to 2011, he was with the Center for Integrated Electronics, Shenzhen Institutes of Advanced Technology, Chinese Academy of Sciences, Shenzhen, China. He is currently an Associate Professor with the School of Electronics and Information Technology, Sun Yat-sen University, Guangzhou, China. His research interests include UAV communications, non-orthogonal multiple access, wireless communications powered by energy harvesting, cooperative communications, and ultra-wideband communications.

QUANZHONG LI received the B.S. and Ph.D. degrees in information and communications engineering from Sun Yat-sen University (SYSU), Guangzhou, China, in 2009 and 2014, respectively.

He is currently an Associate Professor with the School of Data and Computer Science, SYSU. His research interests include UAV communications, non-orthogonal multiple access, wireless communications powered by energy harvesting, cognitive radio, cooperative communications, and multiple-input-multiple-output communications.

JIAYIN QIN received the M.S. degree in radio physics from Huazhong Normal University, Wuhan, China, in 1992, and the Ph.D. degree in electronics from Sun Yat-sen University (SYSU), Guangzhou, China, in 1997.

He was with SYSU as the Head of the Department of Electronics and Communication Engineering, from 2002 to 2004, and the Vice Dean of the School of Information Science and Technology, from 2003 to 2008, where he is currently a Professor with the School of Electronics and Information Technology. His research interests include wireless communications and submillimeter wave technology.

Dr. Qin was a recipient of the IEEE Communications Society Heinrich Hertz Award for the Best Communications Letter, in 2014, the Second Young Teacher Award of Higher Education Institutions, Ministry of Education (MOE), China, in 2001, the Seventh Science and Technology Award for Chinese Youth, in 2001, and the New Century Excellent Talent, MOE, China, in 1999.

• • •